The 24th Conference of the Mechanical Engineering Network of Thailand
October 20 – 22, 2010, Ubon Ratchathani

Comparative performance of evolutionary algorithms on simultaneous topology, shape and sizing optimization of a truss tower

Chaid Noilublao[1] and Sujin Bureerat[1*]

[1] Department of mechanical engineering, Faculty of engineering, Khon Kaen University, Thailand, 40002
*Corresponding Author: sujbur@kku.ac.th

Abstract

This paper presents an integrated design technique to carry out simultaneous topology, shape and sizing optimization of a three-dimensional truss structure. An optimization problem is set to find structural layout, shape, and truss bars' cross-sections such that multiple objective functions including mass, compliance, natural frequencies, frequency response function (FRF), and force transmissibility (FT) are optimised. The Pareto optimal solutions of design testing problems are explored by using two multiobjective evolutionary algorithms (MOEAs) namely strength Pareto evolutionary algorithm (SPEA) and population-based incremental learning (PBIL). The results obtained from using the two optimizers are illustrated and compared. Based upon the hypervolume performance indicator, it is shown that PBIL is superior to SPEA when optimizing compliance and natural frequency, while the latter is superior when dealing with FRF and FT.

Keywords*:* Topology optimization; truss structure; multiobjective evolutionary algorithms; population-based incremental learning; vibration reduction

1. Introduction

In structural optimisation, design variables can be categorised into three groups as topology, shape and sizing variables. Topological design variables determine initial structural layout whereas shape and sizing parameters give the shape and dimensions of structures. Traditionally, a designer performs topological optimization at the first design phase to obtain initial structural configuration. The optimum shape and sizes of the structure are then evaluated in the later design stage. This is often called multi-stage optimisation. Nevertheless, it has been found that the better design process is to perform topology, shape, and sizing optimisation simultaneously. This is easier said than done. The combination of shape and sizing design may be easily carried out but, when combining topological variables to the design task, it is more difficult and complicated. However, such an integrated design approach can be attained and applied to both continuum and skeletal structures.

The applications of such integrated design concept for skeletal structures (trusses and frames) have been studied for many years where both gradient-based and population-based optimizers were used [1-5]. Design problems were mostly limited to single objective. Objective functions usually include structural weight, static and dynamic stiffness. Recent investigation [6] shows that the use of multiobjective evolutionary algorithms for this type of design problem is possible and effective. The work in [6] shows that multiobjective design of simple frames with combined topology, shape, and sizing design variables is achievable. The two best optimizers are real-code strength Pareto evolutionary algorithm and binary-code population-based incremental learning. However, the performance of these two methods in dealing with large-scale practical design has not been studied yet.

This work presents an approach to achieve simultaneous topology, shape and sizing optimization of a three-dimensional truss structure. An optimization problem is set to find structural layout, shape, and truss elements' cross-sectional areas within one simulation run such that optimizing multiple objective functions including mass, compliance, natural frequencies, frequency response function, and force transmissibility. The Pareto optimal solutions are explored by using SPEA and PBIL. The results obtained from using the two optimizers are illustrated and compared.

2. Finite element modelling [6]

Trusses and frames are some of the most commonly used structures in daily life. Using such a structure is said to be advantageous since they are simple and inexpensive to construct. It can be employed in many engineering purposes e.g. transmission towers, wind turbine towers, communication towers, civil engineering structures, and mechanical parts.

A linear structural dynamic model can be thought of as a structure being in a dynamic equilibrium state. It is the state at which the system has minimum potential energy (this includes structural elastic restoration, the work done by external forces, and the work due to inertial forces). By using a finite element approach, the structural dynamic model is represented by

$$\mathbf{M}\ddot{\boldsymbol{\delta}} + \mathbf{K}\boldsymbol{\delta} = \mathbf{F}(t) \tag{1}$$

where $\boldsymbol{\delta}$ is the vector of structural displacements, **M** is a structural mass matrix, **K** is a structural stiffness matrix, and **F** is the vector of dynamic forces acting on the structure.

With the given prescribed displacements (say $\boldsymbol{\delta}_b$ = **0**), Equation (1) can be partitioned as

$$\begin{bmatrix} \mathbf{M}_{aa} & \mathbf{M}_{ab} \\ \mathbf{M}_{ba} & \mathbf{M}_{bb} \end{bmatrix} \begin{bmatrix} \ddot{\boldsymbol{\delta}}_a \\ \ddot{\boldsymbol{\delta}}_b \end{bmatrix} + \begin{bmatrix} \mathbf{K}_{aa} & \mathbf{K}_{ab} \\ \mathbf{K}_{ba} & \mathbf{K}_{bb} \end{bmatrix} \begin{bmatrix} \boldsymbol{\delta}_a \\ \boldsymbol{\delta}_b \end{bmatrix} = \begin{bmatrix} \mathbf{F}_a \\ \mathbf{F}_b \end{bmatrix} \tag{2}$$

where the subscript *b* indicates the known displacements and unknown reactions at the boundary conditions, and the subscript *a* denotes unknown displacements and predefined external forces.

Equation (2) can be rearranged leading to 2 systems of differential equations as:

$$\mathbf{M}_{aa}\ddot{\boldsymbol{\delta}}_a + \mathbf{K}_{aa}\boldsymbol{\delta}_a = \mathbf{F}_a \tag{3}$$

and

$$\mathbf{M}_{ba}\ddot{\boldsymbol{\delta}}_a + \mathbf{K}_{ba}\boldsymbol{\delta}_a = \mathbf{F}_b\,. \tag{4}$$

In the cases of free vibration analysis, Equation (3) can be written as

$$\mathbf{M}_{aa}\ddot{\boldsymbol{\delta}}_a + \mathbf{K}_{aa}\boldsymbol{\delta}_a = \mathbf{0} \tag{5}$$

By substituting $\boldsymbol{\delta}_a = \bar{\boldsymbol{\delta}}_a e^{i\omega t}$ to (5), we have an eigenvalue problem

$$(\mathbf{K}_{aa} - \omega^2 \mathbf{M}_{aa})\bar{\boldsymbol{\delta}}_a = \mathbf{0} \tag{6}$$

Solving such a system of equations leads to N natural frequencies $\boldsymbol{\omega} = \{\omega_1, \omega_2, \ldots, \omega_N\}$ and their corresponding eigenvectors $\boldsymbol{\Phi} = [\boldsymbol{\varphi}_1, \boldsymbol{\varphi}_2, \ldots, \boldsymbol{\varphi}_N]$, where N is the size of the square mass and stiffness matrices. The orthogonality conditions can be expressed as

$$\begin{aligned} \boldsymbol{\Phi}^T \mathbf{M}_{aa} \boldsymbol{\Phi} &= diag(\mu_i) \\ \boldsymbol{\Phi}^T \mathbf{K}_{aa} \boldsymbol{\Phi} &= diag(\mu_i \omega_i^2) \end{aligned} \tag{7}$$

By using the proportional damping concept (also known as Rayleigh damping), a damping matrix can be introduced to the model leading to

$$\mathbf{M}_{aa}\ddot{\boldsymbol{\delta}}_a + \mathbf{C}_{aa}\dot{\boldsymbol{\delta}}_a + \mathbf{K}_{aa}\boldsymbol{\delta}_a = \mathbf{F}_a \tag{8}$$

where $\mathbf{C}_{aa} = \alpha\mathbf{M}_{aa} + \beta\mathbf{K}_{aa}$, and α and β are damping coefficients to be defined.

From equation (8), by substituting $\boldsymbol{\delta}_a = \bar{\boldsymbol{\delta}}_a e^{i\omega t}$ and $\mathbf{F}_a = \bar{\mathbf{F}}_a e^{i\omega t}$, a frequency response function (FRF) matrix can be approximated as [7]

$$\mathbf{H}(\omega) \approx \sum_{i=1}^{m} \frac{\boldsymbol{\varphi}_i \boldsymbol{\varphi}_i^T}{\mu_i(\omega_i^2 - \omega^2 + 2j\xi_i\omega_i\omega)} + \mathbf{K}_{aa}^{-1} - \sum_{i=1}^{m} \frac{\boldsymbol{\varphi}_i \boldsymbol{\varphi}_i^T}{\mu_i \omega_i^2} . \tag{9}$$

Figure 1 illustrates how to measure $H(r,s)$ which represents the ratio of a displacement response at the r^{th} degree of freedom to a harmonic excitation at the s^{th} degree of freedom.

Furthermore, by defining force transmissibility, denoted by $\mathbf{T}(\omega)$, as the ratio of output harmonic reaction forces to the input external harmonic forces, it can be written as

$$\mathbf{T}(\omega) = \left(-\omega^2 \mathbf{M}_{ba} + \mathbf{K}_{ba}\right)\mathbf{H} \tag{10}$$

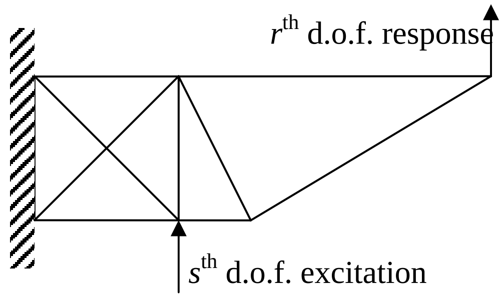

Fig. 1. Measurement of FRF

In reducing structural vibration, FRF and FT determine structural merit. The lower FRF or FT at a particular frequency results in the better structural vibration suppression design. Therefore, a design objective can be assigned in such a way that frequency responses at a frequency range of interest are minimised. Moreover, maximising structural natural frequency is an alternative criterion for design of structures under dynamic loadings.

3. Testing Problems

A three-dimensional truss tower is used for this study. Four testing problems are posed to find the optimum tower shape, bar sizes, and topology such that minimising two objective functions while satisfying design constraints. The integrated topology, shape, and sizing optimisation problem can be expressed as

min $[f_1, f_2]$ (11)

subject to

$$\sigma_{\max} \le \sigma_{\text{all}}$$

$$\lambda_i \le 1$$

$\mathbf{x} \in \Omega$

where f_1, f_2 are objective functions

σ_{max} is the maximum stress on truss elements.

σ_{all} is an allowable stress to be defined

λ_i is a buckling factor of each element (defined as the ratio of applied load to critical load)

x is a vector of design variables

and Ω is a design domain of **x**.

The tower is subject to four static load cases acting at the top with structural weight also being added to the force vectors. The tower is 50-m high with square cross-sectional area. Fig. 2 displays 4 parameters that control the shape of the tower. Having 4 input parameters, the tower can be shaped by using an interpolation technique. The tower is allowed to have 10-20 tower sections. A tower topology can be obtained by using an adaptive ground element approach. Figure 3 shows the ground finite elements of a particular tower section. On each section, there are 8 nodal points, and 16 ground elements. 6 design parameters are assigned as the cross-sectional areas of those elements to maintain structural symmetry as given in Table 1. With the ground finite element approach, elements having too small cross-sectional areas are deleted from the structure. This is a means to define truss topology and, at the same time, to define the elements' cross-sectional areas.

Design variables can be encoded as binary or real parameters. In the decoding process, there are three groups of design variable i.e. the first group determines the number of tower sections, the second group gives the four variables to control tower shape as displayed in Figure 2, and the last group represents ground elements' cross-sectional areas. In the last design variable group, on each tower section, 6 design variables are assigned as the cross-sectional areas of 16 ground elements. In cases that, the area after performing optimisation is too small, the corresponding ground elements will be deleted from the section to form a structural layout. The flowchart for function evaluation is displayed in Figure 4.

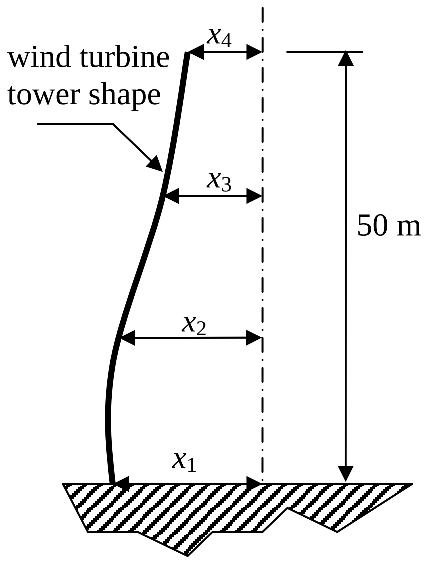

Fig. 2 parameters for defining a tower shape

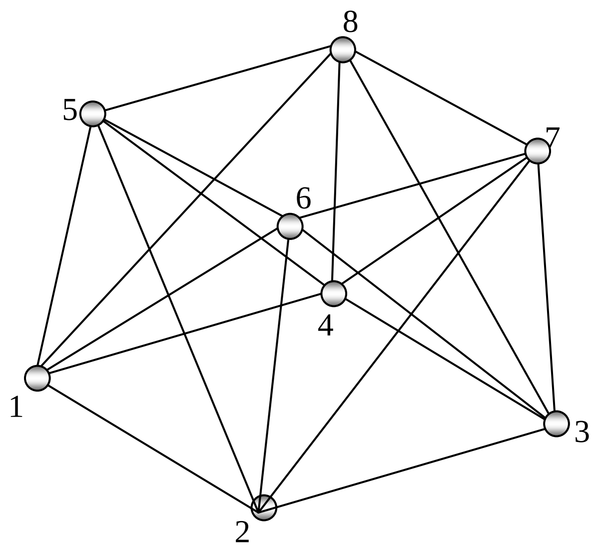

Fig. 3 Ground elements for each tower section

Table 1 Element connectivity and cross-sectional variables.

Elements as node number connections	Cross-sectional areas
1-2 3-4 2-3 4-1	x_1
1-5 2-6 3-7 4-8	x_2
1-6 3-8	x_3
2-5 4-7	x_4
1-8 3-6	x_5
4-5 2-7	x_6

The four bi-objective design problems have the same constraints as shown in Equation (11). The objective functions of each design problems are given as follows:

- OPT1: f_1 = structural mass, f_2 = structural compliance
- OPT2: f_1 = structural mass, f_2 = natural frequencies
- OPT3: f_1 = structural mass, f_2 = mean values of FRF crest parameters
- OPT4: f_1 = structural mass, f_2 = mean values of FT crest parameters

More details of the objective functions are given in [6].

The two optimisers, SPEA (its second version) using real code [8-9] and PBIL [10-11], are implemented to solve the optimisation problems three runs for each problem with the population size of 200, and number of generation as 300. The external Pareto archive size is set to be 200. The performance assessment is carried out by using the well-known hypervolume indicator [12].

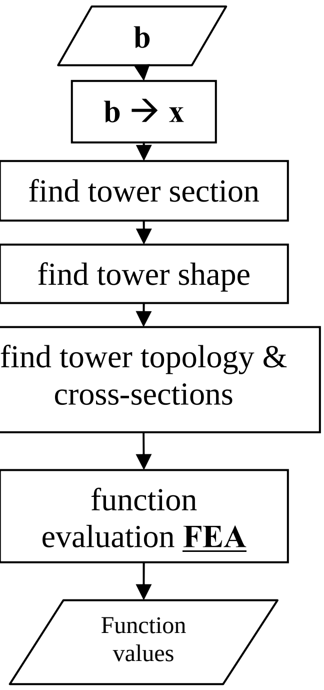

Fig. 4 Flowchart for design variables decoding

4. Results

Having used the multiobjective evolutionary algorithms to tackle the design problems three optimisation runs for each problem, the hypervolumes of the Pareto fronts obtained are evaluated and shown in Table 2. Note that the higher hypervolume the better Pareto front. From the comparative results, it can be seen that the best method for the first design problem OPT1 is PBIL since the average value of front hypervolumes produced by PBIL is higher. The best run for this design problem comes from the third run of PBIL (the bold value). For OPT2, the best optimiser is still PBIL whereas the best run is from the first run of PBIL. SPEA is overall superior to PBIL for OPT3; however, the best run is from the second run of PBIL. Similarly to OPT3, SPEA outperforms PBIL in cases of OPT4 while the best run is the third run of SPEA.

Table 2 Hypervolume values

No. of runs		1	2	3	Avg
OPT1	SPEA	0.77	0.44	0.31	0.50
	PBIL	0.72	0.66	**0.79**	0.72
OPT2	SPEA	0.55	0.70	0.68	0.65
	PBIL	**0.80**	0.78	0.66	0.75
OPT3	SPEA	0.67	0.77	0.85	0.76
	PBIL	0.42	**0.92**	0.75	0.70
OPT4	SPEA	0.94	0.90	**0.99**	0.94
	PBIL	0.25	0.59	0.65	0.50

The best front (from the best run) of OPT1 is displayed in Fig. 5 where some selected design solutions are highlighted. The truss towers corresponding to the selected design solutions in Fig. 5 are shown in Fig. 6. For OPT2, the best front is shown in Fig. 7 while the corresponding structures are illustrated in Fig. 8. The best front of OPT3 is shown in Fig. 9 while the corresponding structures are illustrated in Fig. 10. For the fourth testing problem OPT4, the best front is depicted in Fig. 11 whereas the associated structures are illustrated in Fig. 12. The structures in Fig. 6, 8, 10 and 12 are said to have similar shapes and topologies with various elements' cross-sections.

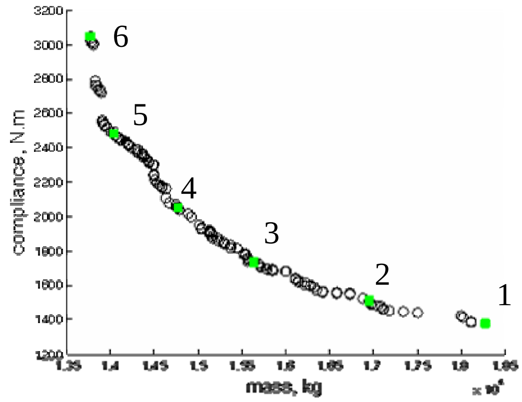

Fig. 5 Best front of OPT1

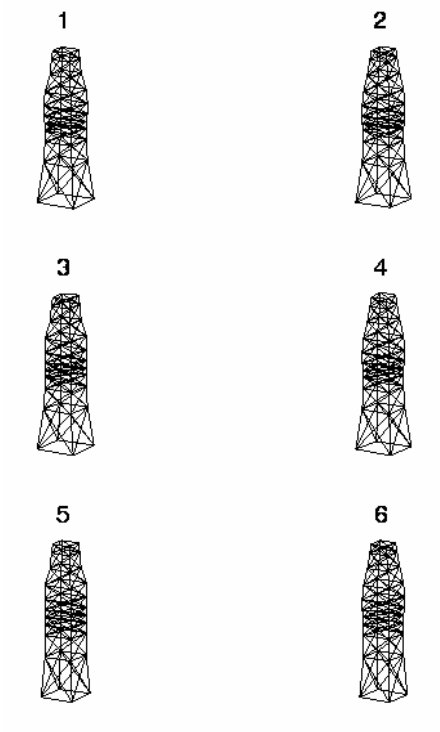

Fig. 6 Structures from the front in Fig. 5

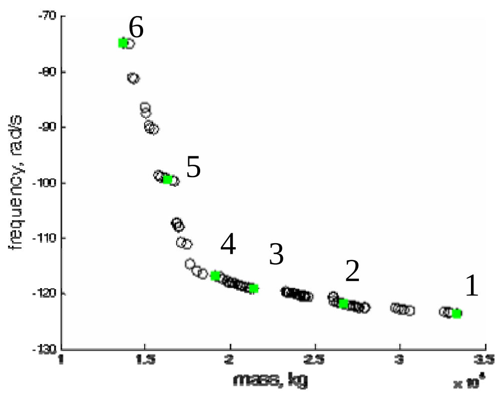

Fig. 7 Best front of OPT2

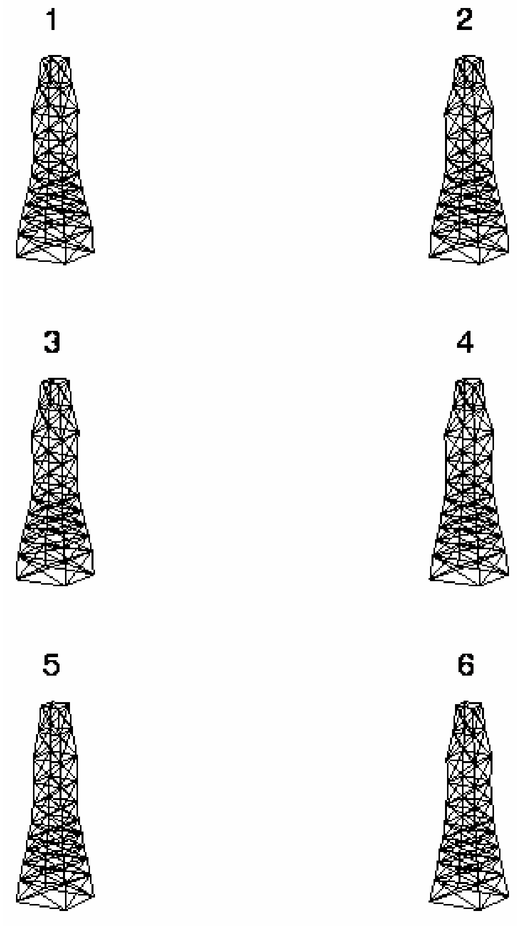

Fig. 8 Structures from the front in Fig. 7

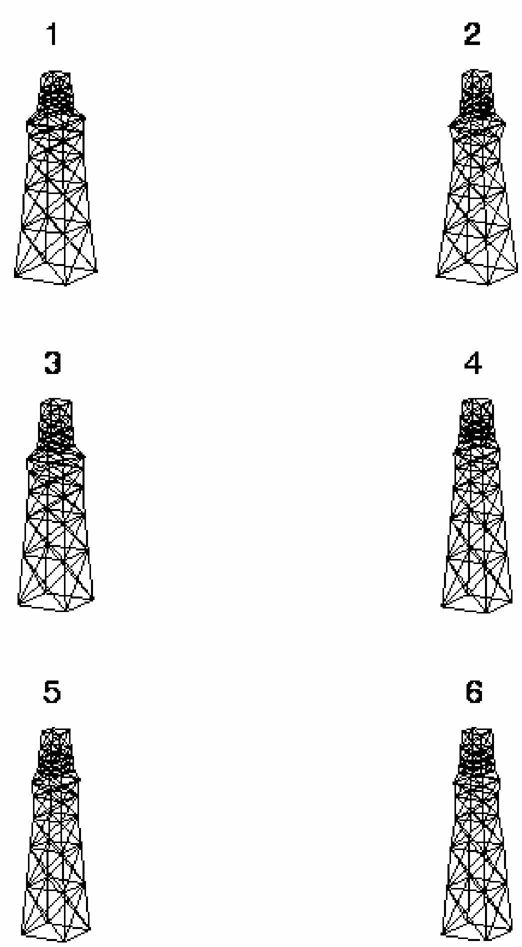

Fig. 10 Structures from the front in Fig. 9

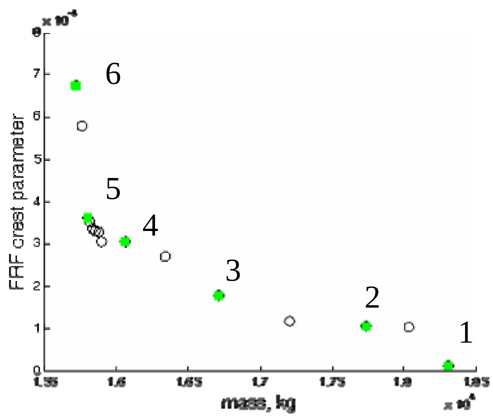

Fig. 9 Best front of OPT3

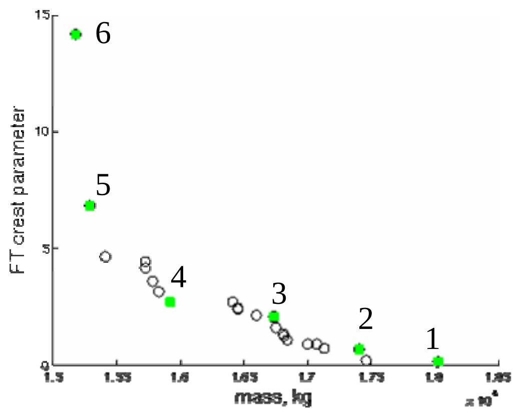

Fig. 11 Best front of OPT4

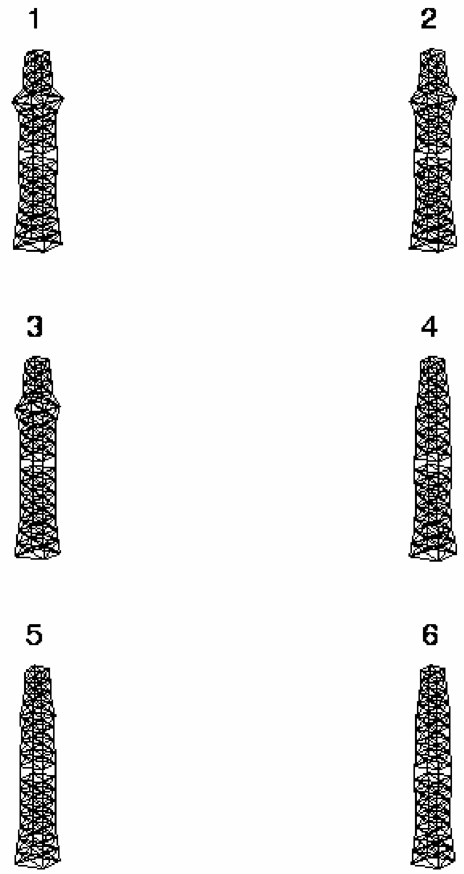

Fig. 12 Structures from the front in Fig. 11

5. Conclusions

From the comparative results, it can be concluded that PBIL is superior when optimising structural compliance (static stiffness) and natural frequencies (dynamic stiffness) while the SPEA method is better when optimising FRF and FT. The obtained truss structure are said to be practical with further detailed design phase. The proposed approach can be a powerful tool for truss and frame design. By using this design strategy, various optimum structures for decision making can be obtained within one simulation run.

6. Acknowledgement

The authors are grateful for the support from the sustainable infrastructure research and development center (SIRDC), Khon Kaen University.

7. References

[1] Wang, X.; Wang, M.Y. and Guo, D. (2004). Structural shape and topology optimization in a level-set-based framework of region representation. *Structural and Multidisciplinary Optimization*, Vol. 27, pp. 1–19.

[2] Tang, W.; Tong, L. and Gu, Y. (2005). Improved genetic algorithm for design optimization of truss structures with sizing, shape and topology variables. *International Journal for Numerical Methods in Engineering*, Vol. 62, No. 13, pp. 1737 – 1762.

[3] Shea, K. and Smith, I.F.C. (2006). Improving full-scale transmission tower design through topology and shape optimization. *Journal of Structural Engineering*, Vol. 132, No. 5, pp. 781–790.

[4] Chan, C.M. and Wong, K.M. (2008). Structural topology and element sizing design optimization of tall steel frameworks using a hybrid OC–GA method. *Structural and Multidisciplinary Optimization*, Vol. 35, pp. 473–488.

[5] Zhu, J.; Zhang, W.; Beckers, P.; Chen, Y. and Guo Z. (2008). Simultaneous design of components layout and supporting structures using coupled shape and topology optimization technique. *Structural and*

Multidisciplinary Optimization, Vol. 36, pp. 29–41.

[6] Noilublao, C. and Bureerat, S., 2009. Simultaneous topology shape and sizing optimisation of skeletal structures using multiobjective evolutionary algorithms. *Evolutionary Computation*, In-Tech, ISBN 978-953-307-008-7, pp. 487-580.

[7] Preumont, A. (2001). *Vibration control of active structures: an introduction*, Kluwer Academic Publishers

[8] Zitzler, E.; Laumanns, M. and Thiele, L. (2002). SPEA2: improving the strength Pareto evolutionary algorithm for multiobjective optimization. paper presented in *Evolutionary Methods for Design, Optimization and Control*, Barcelona, Spain

[9] Srisomporn, S. and Bureerat, S. (2008). Geometrical design of plate-fin heat sinks using hybridization of MOEA and RSM. *IEEE Trans on Components and Packaging Technologies*, Vol. 31, pp. 351-360.

[10] Bureerat, S. and Sriworamas K. (2007). Population-based incremental learning for multi-objective optimisation. *Advances in Soft Computing*, Vol. 39, pp. 223-232

[11] Bureerat, S. and Srisomporn, S. (2010). Optimum plate-fin heat sinks by using a multi-objective evolutionary algorithm, Engineering Optimization, vol. 42, pp. 305-343.

[12] While, L., Hingston, P., Barone, L. and Huband, S. 2006. A Faster algorithm for calculating hypervolume. *IEEE Transaction on Evolutionary Computation*, vol. 10, pp. 29-38.